COMMUNICATIONS IN NUMERICAL METHODS IN ENGINEERING
Commun. Numer. Meth. Engng 2004; **20**:647–653 (DOI: 10.1002/cnm.673)

Conjugate approximation with smoothing for hybrid photoelastic and FEM analysis

Minvydas Ragulskis[1,*,†] and Liutauras Ragulskis[2]

[1]*Kaunas University of Technology, P.O. Box 1300, LT-3028, Kaunas, Lithuania*
[2]*Vytautas Magnus University, Lithuania*

SUMMARY

Meaningful visualization of finite element method (FEM) results is important for building the ground for hybrid numerical–experimental techniques. This is not a straightforward procedure for photoelastic analysis as conventional FEM techniques are based on the approximation of nodal displacements, not stresses. Although the displacements are continuous at inter-element boundaries, the calculated stresses are discontinuous due to the operation of differentiation. Conventional FEM would require unacceptably dense meshing for producing sufficiently smooth photoelastic fringe patterns. Therefore, there exists a need for the development of a technique for smoothing the generated photoelastic fringes representing the stress distribution and calculated from the displacement distribution. The proposed smoothing technique is based on the minimization of the augmented residual. Copyright © 2004 John Wiley & Sons, Ltd.

KEY WORDS: finite elements; conjugate approximation; smoothing; photoelasticity

1. INTRODUCTION

Visualization techniques of the results from finite element analysis procedures are important due to several reasons. First is the meaningful and accurate representation of processes taking place in the analysed structures. Second, and perhaps even more important, is building the ground for hybrid numerical–experimental techniques. A typical example of FEM application in developing a hybrid technique is presented in Reference [1].

Conventional finite element analysis (FEM) analysis techniques are based on the approximation of nodal displacements (not stresses) via the shape functions. Ramesh *et al.* [2] have noted that photoelastic isochromatics can be effectively used for the detection of FEM meshing problems.

Analysis of natural vibrations using dynamic photoelasticity techniques is an attractive methodology evaluating the quality of the structural design in terms of the stress distribution. Conventional FEM would require unacceptably dense meshing for producing sufficiently smooth photoelastic patterns. Therefore, there exists a need for the development of a technique

*Correspondence to: M. Ragulskis, Kaunas University of Technology, P.O. Box 1300, LT-3028, Kaunas, Lithuania.
†E-mail: minvydas.ragulskis@ktu.lt

Received 16 January 2003
Accepted 30 June 2003

for smoothing the generated photoelastic fringe patterns representing the stress distribution and calculated from the displacement distribution. The proposed smoothing technique is a further development of the conjugate approximation used for the calculation of nodal values of stresses [3] and enables one to obtain the photoelastic images of acceptable quality on rather coarse meshes using the displacement formulation for the calculation of the eigenmodes.

On the other hand, it can be mentioned that the developed techniques build the ground for hybrid numerical–experimental photoelastic analysis.

2. CONJUGATE APPROXIMATION WITH SMOOTHING IN PHOTOELASTIC ANALYSIS

The eigenmodes for the structure in the state of plane stress are calculated by using the displacement formulation common in the finite element analysis [4, 5]. It is assumed that the structure performs high-frequency vibrations according to the eigenmode. The vibrations of the structure are registered stroboscopically when the structure is in the state of extreme deflections. In this case, the problem is to obtain the nodal stresses of acceptable quality for the eigenmode (the eigenmode of stresses), which are further used for the calculation of the photoelastic images.

The stresses at the points of numerical integration of the finite element are calculated in the usual way:

$$\begin{Bmatrix} \sigma_x \\ \sigma_y \\ \tau_{xy} \end{Bmatrix} = [D][B]\{\delta_0\} \tag{1}$$

where $\{\delta_0\}$ is the vector of nodal displacements of the eigenmode; $[B]$ is the matrix relating the strains with the displacements; $[D]$ is the matrix relating the stresses with the strains; $\sigma_x,\ \sigma_y,\ \tau_{xy}$ are the components of the stresses in the problem of plain stress. The displacements are continuous at inter-element boundaries, but the calculated stresses are discontinuous due to the operation of differentiation.

The appropriate eigenmode of stresses is obtained by minimizing the following augmented residuals:

$$\begin{aligned} &\frac{1}{2}\iint \left(([N]\{\delta_x\} - \sigma_x)^2 + \lambda \left(\left(\frac{\partial \sigma_x}{\partial x}\right)^2 + \left(\frac{\partial \sigma_x}{\partial y}\right)^2 \right) \right) \mathrm{d}x\,\mathrm{d}y \\ &\quad = \frac{1}{2}\iint (([N]\{\delta_x\} - \sigma_x)^2 + \lambda \{\delta_x\}^{\mathrm{T}}[B^*]^{\mathrm{T}}[B^*]\{\delta_x\})\,\mathrm{d}x\,\mathrm{d}y \\ &\qquad \frac{1}{2}\iint (([N]\{\delta_y\} - \sigma_y)^2 + \lambda \{\delta_y\}^{\mathrm{T}}[B^*]^{\mathrm{T}}[B^*]\{\delta_y\})\,\mathrm{d}x\,\mathrm{d}y \\ &\qquad \frac{1}{2}\iint (([N]\{\delta_{xy}\} - \tau_{xy})^2 + \lambda \{\delta_{xy}\}^{\mathrm{T}}[B^*]^{\mathrm{T}}[B^*]\{\delta_{xy}\})\,\mathrm{d}x\,\mathrm{d}y \end{aligned} \tag{2}$$

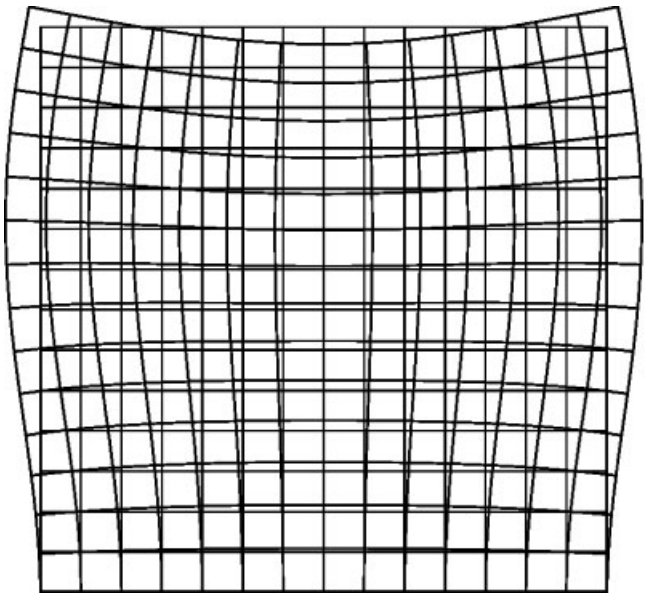

Figure 1. The sixth eigenmode of the cantilever plate (grey lines—the structure in equilibrium, black lines—the eigenmode).

where λ is the smoothing parameter; $\{\delta_x\}$ the global vector of nodal values of σ_x; $\{\delta_y\}$ the global vector of nodal values of σ_y; $\{\delta_{xy}\}$ the global vector of nodal values of τ_{xy}; $[N]$ the row of the shape functions of the finite element; and $[B^*]$ the matrix of the derivatives of the shape functions:

$$[B^*] = \begin{bmatrix} \dfrac{\partial N_1}{\partial x} & \dfrac{\partial N_2}{\partial x} & \cdots \\ \dfrac{\partial N_1}{\partial y} & \dfrac{\partial N_2}{\partial y} & \cdots \end{bmatrix}$$

It must be noted that the integration operators include integrations over the elements and the direct stiffness procedure [4].

The previously mentioned concept of the eigenmode of stresses is understood as the set of vectors $\{\delta_x\}$, $\{\delta_y\}$, $\{\delta_{xy}\}$. The following systems of linear algebraic equations for the determination of each of the components of the stresses are found from Equation (2):

$$\begin{aligned} \iint ([N]^{\mathrm{T}}[N] + [B^*]^{\mathrm{T}}\lambda[B^*])\,\mathrm{d}x\,\mathrm{d}y\{\delta_x\} &= \iint [N]^{\mathrm{T}}\sigma_x\,\mathrm{d}x\,\mathrm{d}y \\ \iint ([N]^{\mathrm{T}}[N] + [B^*]^{\mathrm{T}}\lambda[B^*])\,\mathrm{d}x\,\mathrm{d}y\{\delta_y\} &= \iint [N]^{\mathrm{T}}\sigma_y\,\mathrm{d}x\,\mathrm{d}y \\ \iint ([N]^{\mathrm{T}}[N] + [B^*]^{\mathrm{T}}\lambda[B^*])\,\mathrm{d}x\,\mathrm{d}y\{\delta_{xy}\} &= \iint [N]^{\mathrm{T}}\tau_{xy}\,\mathrm{d}x\,\mathrm{d}y \end{aligned} \tag{3}$$

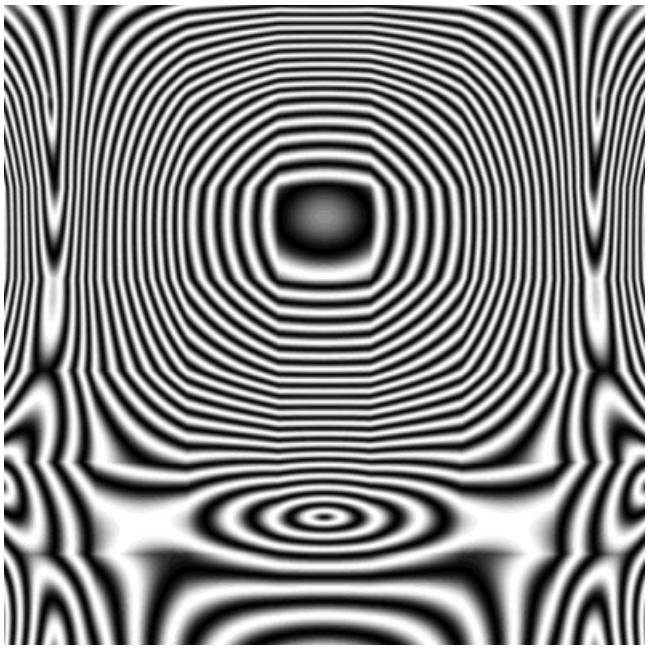

Figure 2. Isochromatics (the image produced by the circular polariscope) without smoothing for the sixth eigenmode.

The choice of the smoothing parameter is performed interactively from the qualitative view of the digital photoelastic images. When the parameter is too small the images are of unacceptable quality because of the unphysical behaviour of the stress field as a result of their calculation from the displacement formulation. When the parameter is too big an over-smoothed image is obtained which may look acceptable but be far from the real photoelastic image. So the best value of the parameter might be considered when most of the image is of acceptable quality without the unphysical behaviour produced by the approximation.

The smoothing parameter can be interpreted as a small penalty parameter to prevent the growth of derivatives of each component of the stresses. This is explicitly shown in Equation (2) where parameter λ defines the magnitude of the augmentation of the residual.

Equation (3) represents three static finite element problems (a separate linear algebraic problem for each component of the stresses). The solution procedure of those equations is numerically effective as the three system matrixes are the same.

The principal stresses σ_1, σ_2 are calculated as the eigenvalues of the matrix:

$$\begin{bmatrix} \sigma_x & \tau_{xy} \\ \tau_{xy} & \sigma_y \end{bmatrix} \tag{4}$$

and the normalized eigenvectors of this matrix $\{V_1\}$, $\{V_2\}$ are the directions of the principal stresses.

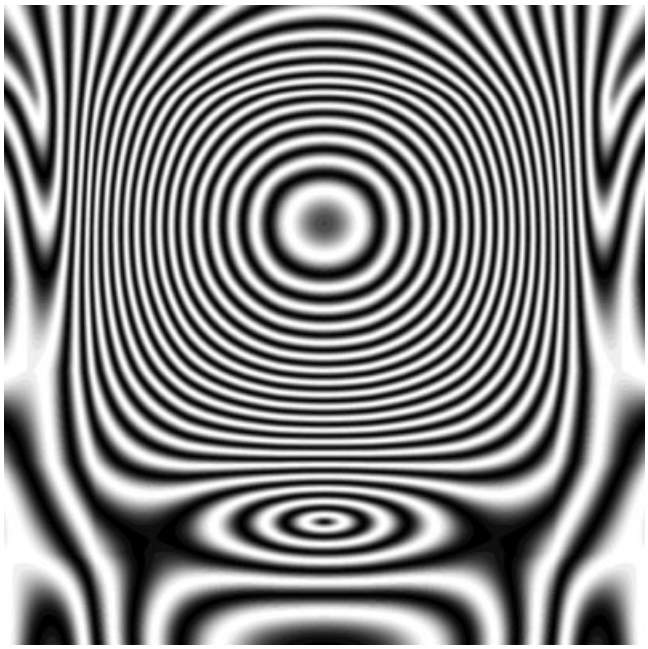

Figure 3. Isochromatics (the image produced by the circular polariscope) with smoothing for the sixth eigenmode.

The vector of polarization is assumed to be given as

$$\{P\} = \begin{Bmatrix} \cos \alpha \\ \sin \alpha \end{Bmatrix} \tag{5}$$

where α is the angle of the vector of polarization with the x-axis.

Then the intensity in the photoelastic image of the plane polariscope (isoclinics and isochromatics intertwined) is calculated as

$$I = (\{\{V_1\}\{P\}\}(\{V_2\}\{P\}) \sin C(\sigma_1 - \sigma_2))^2 \tag{6}$$

where C is the constant dependent on the thickness of the analysed structure in the state of plane stress and on the material from which it is produced [6].

The intensity of the photoelastic image for the circular polariscope (isochromatics) is calculated as

$$I = (\sin C(\sigma_1 - \sigma_2))^2 \tag{7}$$

The plotting scheme used to visualize the results of calculations is described in detail in Reference [7].

The presented methodology is in general also valid for a static case. The only difference is that the solution of the static finite element problem using the conventional displacement

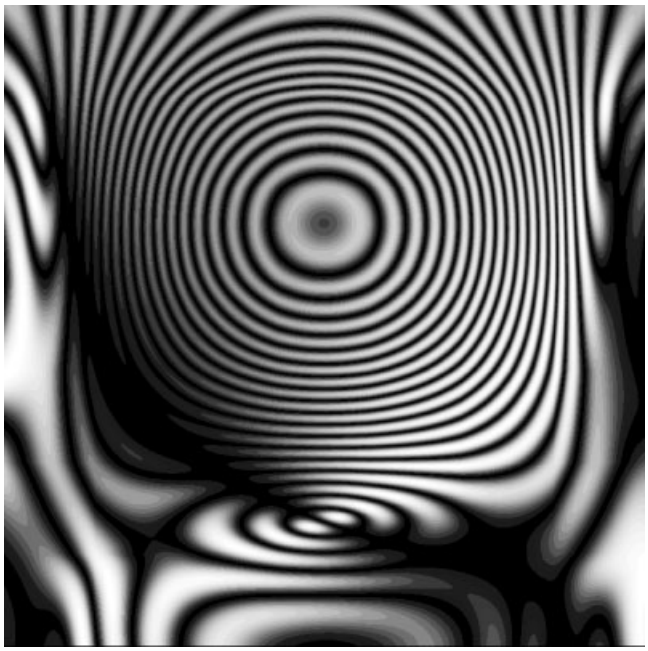

Figure 4. Isoclinics and isochromatics intertwined (the image produced by the plane polariscope) with smoothing for the sixth eigenmode at $\alpha = 3\pi/8$.

formulation should be used instead of the displacements of the appropriate eigenmode. But one is to have in mind that different values of λ may be preferable for different parts of the image when the problems of stress concentration are analysed (larger values of λ in the regions of higher stress concentrations).

3. NUMERICAL RESULTS

The rectangular cantilever plate with a fixed edge in the state of plane stress is analysed. The sixth eigenmode of the plate is shown in Figure 1. The reconstructed image for the circular polariscope (isochromatics) without smoothing is shown in Figure 2.

The same image with smoothing is shown in Figure 3.

The image for the plane polariscope (isoclinics and isochromatics intertwined) when $\alpha = 3\pi/8$ is presented in Figure 4.

The unsmoothed image corresponds to the value of $\lambda = 0$, while the smoothed images presented in Figures 3 and 4 were produced using $\lambda = 0.2$.

In order to illustrate the applicability of the presented methodology for statical problems the same rectangular plate with fixed lower and upper edges in the state of plane stress is analysed. The constant displacement of the upper edge in the downward direction is prescribed. The reconstructed image for the circular polariscope (isochromatics) with smoothing ($\lambda = 0.2$) is presented in Figure 5.

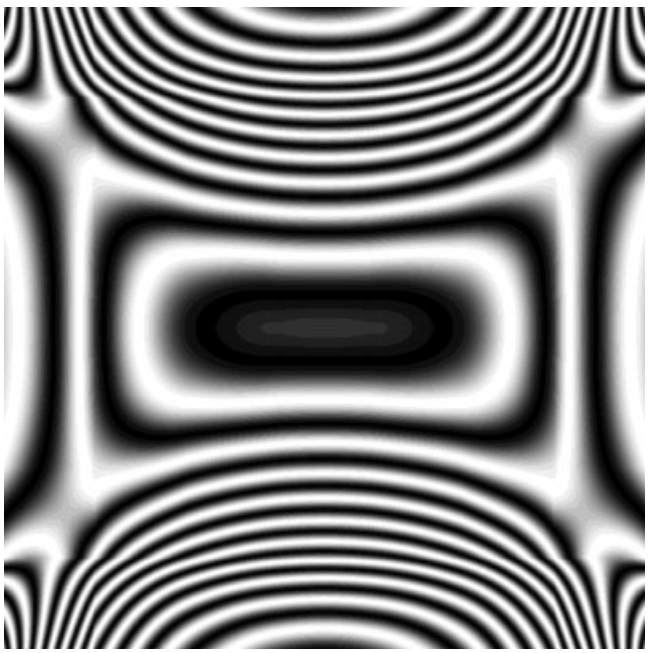

Figure 5. Isochromatics (the image produced by the circular polariscope) with smoothing for the static problem.

4. CONCLUSIONS

The construction of digital photoelastic images builds the ground for hybrid numerical–experimental photoelastic analysis. The displacement-based FEM formulation is coupled with stress-based photoelasticity analysis. The introduced smoothing procedure enables the generation of photoelastic images on rather coarse conventional finite element meshes.

REFERENCES

1. Holstein A, Salbut L, Kujawinska M, Juptner W. Hybrid experimental–numerical concept of residual stress analysis in laser weldments. *Experimental Mechanics* 2001; **41**(4):343–350.
2. Ramesh K, Pathak PM. Role of photoelasticity in evolving discretization schemes for FE analysis. *Journal of Experimental Techniques* 1999; **23**(4):36–38.
3. Segerlind LJ. *Applied Finite Element Analysis*. Mir: Moscow, 1979.
4. Zienkiewicz OC, Morgan K. *Finite Elements and Approximation*. Mir: Moscow, 1986.
5. Bathe KJ. *Finite Element Procedures in Engineering Analysis*. Prentice-Hall, New Jersey, 1982.
6. Timoshenko SP, Goodier JN. *Theory of Elasticity*. Nauka: Moscow, 1975.
7. Ragulskis M, Palevicius A, Ragulskis L. Plotting holographic interferograms for visualization of dynamic results from finite-element calculations. *International Journal for Numerical Methods in Engineering* 2003; **56**: 1647–1659.

